Journal of Current Science and Technology, May-August 2023 Vol. 13 No. 2, pp. 237-250

ISSN 2630-0656 (Online)

Cite this article: Subavathy, P., & Jothi Grace, G. A. (2023, May). Biogenic synthesis, characterization and applications of Tellurium nanoparticles from *Chicoreus virgineus* (Roding, 1798). *Journal of Current Science and Technology*, *13*(2), 237-250. https://doi.org/10.59796/jcst.V13N2.2023.1742

Journal of Current Science and Technology

Journal homepage: https://jcst.rsu.ac.th

Biogenic synthesis, characterization and applications of Tellurium nanoparticles from *Chicoreus virgineus* (Roding, 1798)

P. Subavathy[1*, 3] and G. Amala Jothi Grace[2, 3]

[1]PG and Research Department of Zoology, St. Mary's College (Autonomous), Thoothukudi 628001, Tamil Nadu, India
[2]Department of Chemistry, St. Mary's College (Autonomous), Thoothukudi 628001, Tamil Nadu, India
[3]Manonmaniam Sundaranar University, Abishekapatti, Tirunelveli 627012, Tamil Nadu, India.

[*]Corresponding author; E-mail: subavathy.p89@gmail.com

Received 30 October 2022; Revised 23 December 2022; Accepted 10 January 2023; Published online 15 July 2023

Abstract

Nanoparticles will offer a better perspective for the biogenic manner of the future. The green material's reducing agents offer a crucial pathway for the synthesis of metal nanoparticles. A biological method was adopted to develop tellurium mediated nanoparticles with the shell of marine gastropod *Chicoreus virgineus*. 10.7 g of Tellurium tetrachloride was dissolved in 1 L of the double distilled water to prepare 0.01 M Solution.The nanoparticle synthesis was confirmed by UV-Visible spectroscopy, the absorbance values of the nanoparticles generated were identified and the wavelength around 300nm was observed. The presence of reducing agents is indicated by Fourier Transform Infrared Spectroscopy. FTIR analysis showed the peak values from 3336.35 cm^{-1} to 708.30 cm^{-1}. Images from atomic force microscopy and scanning electron microscopy were used to display the surface morphology. The rod like structure and spherical, uniform shape of tellurium nanoparticles were observed. The particle size of 21.31 nm was recorded for the synthesized nanoparticles. The antibacterial, antifungal, DPPH scavenging, and hydrogen peroxide scavenging assay activity of the produced nanoparticles was tested. The maximum zone of inhibition was observed against the pathogens viz., *Propionibacterium acnes* (6.5 mm) and *Aspergillus fumigatus* (16.5 mm). The highest percentage inhibition of 71.4% for DPPH scavenging activityand 92.12% for hydrogen peroxide assay were observed. Theoutcomes demonstrated that this affordable synthesis found many useful biomedical applications. The current investigation is one of the eco-friendly methods of synthesis and it is an easy method for the synthesis of nanoparticles. These nanoparticles act as an effective antibacterial, antifungal and antioxidant agent. Hence it will show a greater scope in the medicinal field. The nanoparticles derived from marine gastropod *Chicoreus virgineus* has good biocompatibility. Only few studies have been reported earlier using the marine molluscs. This Tellurium nanoparticles from *Chicoreus virgineus* is a new approach to the greener way of synthesis. This highlighted synthesis of Tellurium nanoparticles from sea shell is a new method which provides more applications.

Keywords**:** *antibacterial; antifungal; antioxidant activities; atomic force microscopy; Chicoreus virgineus; tellurium nanoparticle; UV-visible spectroscopy*

1. Introduction

One of the most frequently employed technologies in translational research is nano-technology. Significant interest has been shown in the creation of metallic nanoparticles using biological components in an environmentally

acceptable manner. Algae, cyanobacteria, actinomycetes, bacteria, viruses, yeasts, fungi, and plants are examples of prokaryotic and eukaryotic living things that can be involved in advanced nanotechnology when combined with biology. The capacity of each biological system to produce metallic nanoparticles differs. As a result, bio-reduction particles that result in the manufacture of nanoparticles are utilised to create metallic nanoparticles using biological entities or their extracts. Pharmaceutical uses for these biosynthesized metallic nanoparticles include the administration of medications or genes, the detection of infections or proteins and tissue engineering (Zhang, Ma, Gu, Huang, & Zhang, 2020).

Only a few studies have provided reliable information on the biological activities of the obtained green-synthesized nanomaterials, highlighting the differences of nanoparticle action in various biological host systems, despite the growing interest in the synthesis of nanoparticles using biological methodologies over the past ten years. Tellurium has unique features that have sparked researchers' significant interest in creating Tellurium nanoparticles. The marine molluscan shell *Chicoreus virgineus* is composed of calcium carbonate, as aragonite or calcite, deposited within an organic matrix and also it contains proteins, peptides, lipids and carbohydrates. The calcium carbonate in the shell supports and protects them from predators. The shell of marine mollusc *C. virgineus* is used in the preparation of therapeutically lead bioactive compounds and it form the basis for some rare traditional medicines. The common name of *Chicoreus virgineus* is Virgin Murex. Synthesis by greener way is an easy method and it is unpolluting method in the research field. But the storage and implementation of nanoparticles is still a tough task for researchers. In the current investigation, tellurium nanoparticles were synthesized from the marine molluscan shell *Chicoreus virgineus* (Roding, 1798) and analyzed for antimicrobial and antioxidant activities.

2. Objectives

One of the easiest, most practical, cost-effective, and environmentally benign approaches for creating nanoparticles is employing biological extract. By using biological extracts, the issue can be solved by applying green synthesis techniques to create nanoparticles from natural sources. So, the present study has been carried with the following objectives: To synthesize and characterize the tellurium nanoparticles from marine molluscan shell *Chicoreus virgineus*. And to analyze the antibacterial, antifungal and antioxidant activities of tellurium mediated nanoparticles from *Chicoreus virgineus.*

3. Materials and methods

3.1 Sample collection

In the present study the gastropod *Chicoreus virgineus* was collected from the Gulf of Mannar, Thoothukudi coastal region. The gastropod was collected from the landed by-catch from fishing trawlers operated for crabs and prawns along the Thoothukudi coastal region. The freshly collected samples were brought to the laboratory, cleaned and washed with fresh sea water to remove all impurities. The shells were broken, tissues were removed and the broken shells were dried in hot air oven at 56^{o}C for 48 hours and used for further studies. Approximately 5g of shell powder was immersed into aqueous solvent. The aqueous extract was filtered twice using Whatman No.1 filter paper. Then it was used for the present study.

3.2 Synthesis of Tellurium nanoparticles

Synthesis of Tellurium nanoparticles is carried out using 0.01 M Tellurium chloride in double-distilled water using *Chicoreus virgineus*. Tellurium chloride and the shell extract of *Chicoreus virgineus* were mixed together in a ratio of (9:1, 8:2, 7:3, 6:4, and 5:5). In this different ratio concentration, a 5:5 ratio concentration was selected for the bulk preparation because it shows a higher production than other ratios stirred at 800 rpm using a magnetic stirrer. The mixture turned into milk-white color within 1 hr. The whole reaction was carried out in the dark. The obtained suspension was centrifuged at 15,000 rpm for 15 min. The pellet containing tellurium nanoparticles was washed 3–4 times with deionized water to remove impurities. The precipitated nanoparticles were lyophilized. Lyophilized nanoparticles were stored in a cool, dry and dark place and further characterization was carried out.

3.3 Characterization of Tellurium nanoparticles

UV-absorption spectra of synthesized tellurium nanoparticles by *Chicoreus virgineus* was measured using UV- Visible spectrometer (Shimadzu UV-2700). The functional group present

in the synthesized tellurium nanoparticles was determined using FTIR spectroscopy (Bio-read FTIR 8400S models, USA). The Atomic Force Microscopy analysis was carried out using the Nanosurf easy2 scan BT02218 is profilometer. Scanning Electron Microscopy (SEM) analysis of synthesized tellurium nanoparticles was done using a Hitachi S-4500 SEM machine.X-ray diffraction (XRD) patterns were recorded by a Philips-X'PertPro, X-ray diffractometer using Ni-filtered Cu Kα radiation at scan range of $10<2\theta<80$.

3.4 Antibacterial activity of Te nanoparticles

The antibacterial activity was done following the Agar Well Diffusion Method. Petri plates containing 20 mL nutrient agar medium were seeded with 24hr culture of bacterial strains (*Propionibacterium acnes and Streptococcus oralis*). Wells were cut and different concentrations of sample (500 µg/mL, 250 µg/mL, 100 µg/mL and 50µg/mL) were added. The plates were then incubated at 37°C for 24 hours. The antibacterial activity was assayed by measuring the diameter of the inhibition zone formed around the wells. Gentamicin antibiotic was used as a positive control. The values were calculated using Graph Pad Prism 6.0 software (USA) (De Magaldi, & Camero, 1997).

3.5 Antifungal activity of Te nanoparticles

The antifungal activity was done following the Agar Well Diffusion Method. Petri plates containing 20 mL potato dextrose agar medium was seeded with 72 hr culture of fungal strain (*Cryptococcus neoformans and Aspergillus fumigatus*) wells were cut and different concentration of tellurium nanoparticle (500, 250, 100 and 50 µg/mL) was added. The plates were then incubated at 28°C for 72 hours. The anti-fungal activity was assayed by measuring the diameter of the inhibition zone formed around the wells. Amphotericin B was used as a positive control. The values were calculated using Graph Pad Prism 6.0 software (De Magaldi, & Camero, 1997).

3.6 Antioxidant activity of Te nanoparticles

3.6.1 DPPH radical scavenging activity

The methodology described by Gülcin (2006) was used with slight modifications in order to assess the DPPH free radical scavenging capacity. 0.1 mM of DPPH solution in methanol was prepared and 100µl of this solution was added to 300µl of the solution of sample at different concentrations (500, 250, 100, 50 and 10 µg/mL). The mixtures were shaken vigorously and allowed to stand at room temperature for 30 minutes. Then the absorbance was measured at 517 nm using a UV-VIS spectrophotometer (Ascorbic acid was used as the reference). Lower absorbance values of reaction mixture indicate higher free radical scavenging activity. The capability of scavenging the DPPH radical can be calculated by using the following formula:

DPPH scavenging effect=

$$\frac{\text{Absorbance of control-Absorbance of rxn mixture}}{\text{Absorbance of control}} \times 100$$

Note: rxn = reaction

3.6.2 Hydrogen peroxide scavenging assay

The scavenging ability of hydrogen peroxide was estimated according to the method reported by Ruch, Cheng, & Klaunig (1989) with minor modification. A solution of hydrogen peroxide (43 mM) is prepared in phosphate buffer (1 M pH 7.4). Different concentration of tellurium nanoparticles (500, 250, 100, 50 and 10 µg/mL) was added to hydrogen peroxide solution (0.6 mL, 43 mM). Absorbance of hydrogen peroxide at 230 nm was determined after 10 minutes against a blank solution containing phosphate buffer without hydrogen peroxide. Ascorbic acid was used as standard.

$$\text{Percentage Inhibition} = [(\text{Control-Test})/\text{Control}] \times 100$$

4. Results and discussion

4.1 UV-Visible spectroscopic analysis

In *C.virgineus* the wavelength obtained between 300 nm and 350 nm suggested the presence of tellurium nanoparticles in the solution (Figure 1). This is the specific wavelength which indicates synthesized tellurium nanoparticles. The maximum absorption was obtained between 300 nm and 350 nm. The occurrence peak at absorption intensity from 200 to 600 nm indicated the presence of surface plasmon resonance. Cui et al., (2018) analyzed the production of monodispersed and stable SeNPs from hawthorn fruit extract (HE-SeNPs) and its anticancer action was demonstrated against HepG2 cells by the excess generation of intracellular ROS and loss or disruption of

mitochondrial membrane potential (MMP). Garlic or *Allium sativum*, has the ability to digest chalcogens and produce the metabolites Te-methyltellurocysteine (MeTe-Cys) and S-methyltellurosulfide (Tanaka et al., 2020). Figueroa et al., (2018) reportedthe synthesis of Se and Te nanostructures both *in vivo* and *in vitro* utilising 47 different bacterial strains of *Acinetobacter schindleri* and *Staphylococcus sciuri*. Few works have been published on the biosynthesis of TeNPs using microorganisms (Lian et al., 2019; Wang et al., 2019; Choi et al., 2019). Bartosiak, Giersz, and Jankowski (2019) using continuous photochemical vapour generation (PCVG) in conjunction with microwave-induced plasma optical emission spectrometry (MIP-OES) and UV-Vis spectrophotometry, the precise yield of SeNP synthesis mediated by *Saccharomyces boulardii* was determined (PCVG-MIP-OES). Diko et al. (2020) reported employing *Trichoderma* sp. WL-Go supernatant in culture broth to create spherical and pseudospherical SeNPs. Liang et al. (2020) synthesized SeNPs and TeNPs from four different fungi, including *Aureobasidium pullulans*, *Mortierella humilis*, *Trichoderma harzianum* and *Phoma glomerata* and supplied nucleation sites with extracellular protein and polymeric materials.

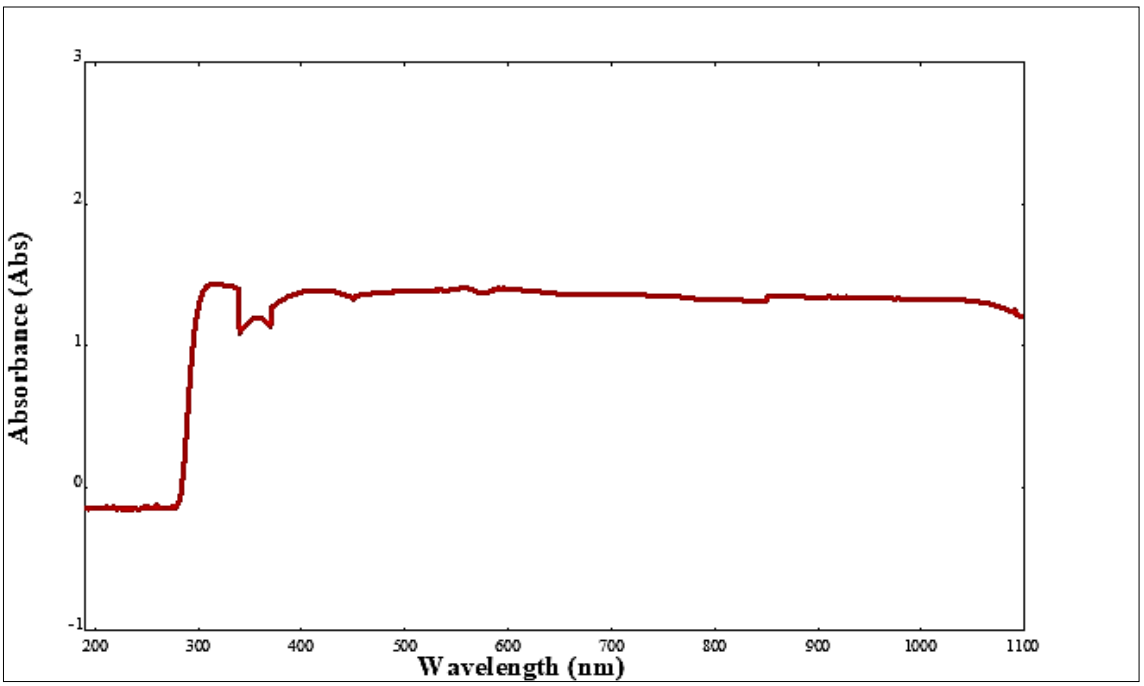

Figure 1 UV-Visible Spectra of Tellurium Nanoparticles using *Chicoreus virgineus*

4.2 Fourier Transform Infra Red (FT-IR) spectroscopic analysis

The results of FTIR analysis of this study show different stretches of bonds shown at different peaks; 3336.35, 1649.92, 1422.23, 1372.06, 1306.46, 1167.53, 1113.50, 905.11, 708.30 cm^{-1}. The image shows a strong absorption peak around 3336.35 cm^{-1} to 1422.23 cm^{-1} which shows the presence of C-H stretching vibration. A peak around 900 cm^{-1} to 1100 cm^{-1} shows the presence of C-O stretching frequency (Figure 2).

Jawad, and Hassan (2021) analyzed the FTIR spectra of NiO nanoparticles showed broad absorption band centered at 3440 cm^{-1} which is attributable to theband O–H stretching vibrations and weak band near 1635 cm^{-1} being assigned to H–O–H bending.

In the meantime, it is suggested that hydroxyl was present in the precursor, and the broad absorption at 767 cm^{-1} is attributed to bond C=O stretching vibrations. The O-C=O symmetric and asymmetric stretching vibrations as well as the C-O stretching vibration are responsible for the

serrated absorption bands in the range of 1000-1500 cm^{-1}. Estevam et al., (2017) generated SeNPs with *Staphylococcus carnosus* TM300, which were isolated by first ultrasonically dissolving the pellet and then centrifuging the NPs separately. Fernández-Llamosas, Castro, Blázquez, Díaz, and Carmona (2016) found that in its stationary growth phase, the anaerobic beta-proteobacteria *Azoarcus* sp. CIB synthesises electron-dense SeNPs and is tolerant to selenite oxyanions. Tugarova, Mamchenkova, Khanadeev, & Kamnev (2020) suggested a general mechanism for *Aspergillus brasiliense* SeNP production.El-Sayyad, El-Bastawisy, Gobara, and El-Batal (2020) *Penicillium chrysogenum* filtrate or *P. chrysogenum* filtrate combined with gentamicin medication (CN) as the stabilising agent following application of irradiation were two alternative environmentally friendly green synthetic techniques used to create SeNPs. The maximum synthesis yield and improved antipathogenic and antibiofilm capabilities were obtained from the second phase. The production of Se-based nanocomposites is likewise simple.

4.3 Atomic Force Microscopy

AFM technique is the one of the best tools for measuring nano sized materials. An AFM topographical image of tellurium nanoparticles is shown in Figure 3 which shows the rod like structure. The average length of the rod structure is in 16.2 nm. It may be due to the metal bindings. In the present study AFM images of tellurium nanoparticles showed average roughness of 2817.1 pm, root mean square is 3.801 nm. Jawad, and Hassan (2021) reported the typical AFM images of the NiO nanoparticles, it shows images measured with size = 2032 x 2027 nm, and ability analytical pixel = 392, 392. AFM images in three dimensions (3D), explainthe structure shape for grain. In two dimensions (2D), images it is found that average roughness is (0.311 nm). The Root mean square (RMS) is (0.3581 nm). The average particle size is 41.13 nm and also indicated that 10%, 50% and 90% of the prepared nano NiO have a particle size being less than 34 nm, 44 nm and 48 nm respectively. Hu et al. (2018) established that SeNPs were bioavailable in the roots and shoots, where they could be biotransformed into organic selenium compounds, selenite and selenate, to produce plants that were Se-biofortified. Several papers have reported the plant-derived biosynthesis of SeNPs with varying sizes and morphologies. Lian et al. (2019) observed Magnusiomyces ingens LH-F1 yeast cell-free extract was used to generate spherical and quasi-spherical SeNPs that ranged in size from 70 to 90 nm. Some surface proteins were crucial to the process, functioning as capping or reducing agents.

4.4 SEM analysis

SEM analysis shows high-density tellurium nanoparticles synthesized by *C. virgineus* shell extract (Figure 4). It was shown that relatively spherical and uniform tellurium nanoparticles were formed with diameter of 219.7 nm to 657.0 nm. The SEM image of tellurium nanoparticles was due to interactions of hydrogen bond and electrostatic interactions between the bioorganic capping molecules bound to the tellurium nanoparticles. By manually measuring and counting the particles or by utilizing specialised software, we may use SEM to examine the morphology of the particles and generate a histogram from the images (Fissan, Ristig, Kaminski, Asbach, & Epple, 2014). Spherical, triangular, and hexagonal SeNPs with a size of 20–50 nm was produced by *Hibiscus sabdariffa* (Fan et al., 2020). while crystalline, spherical, smooth-surfaced SeNPs have been made quickly and effectively by using *Azadirachta indica* (Mulla, Otari, Bohara, Yadav, & Pawar, 2020).

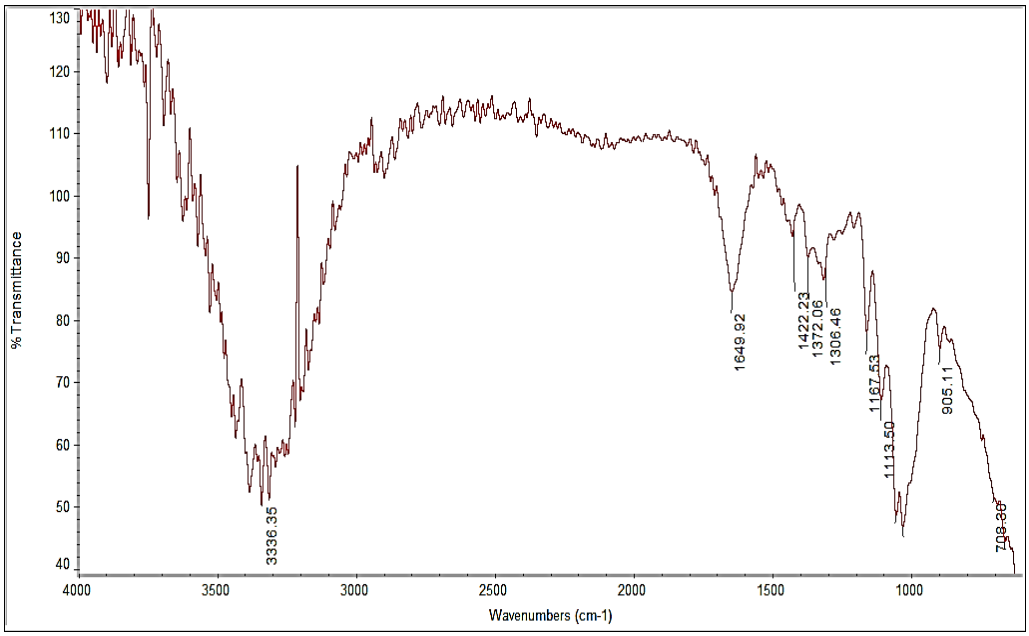

Figure 2 Infra Red Spectra of Tellurium Nanoparticles using *Chicoreus virgineus*

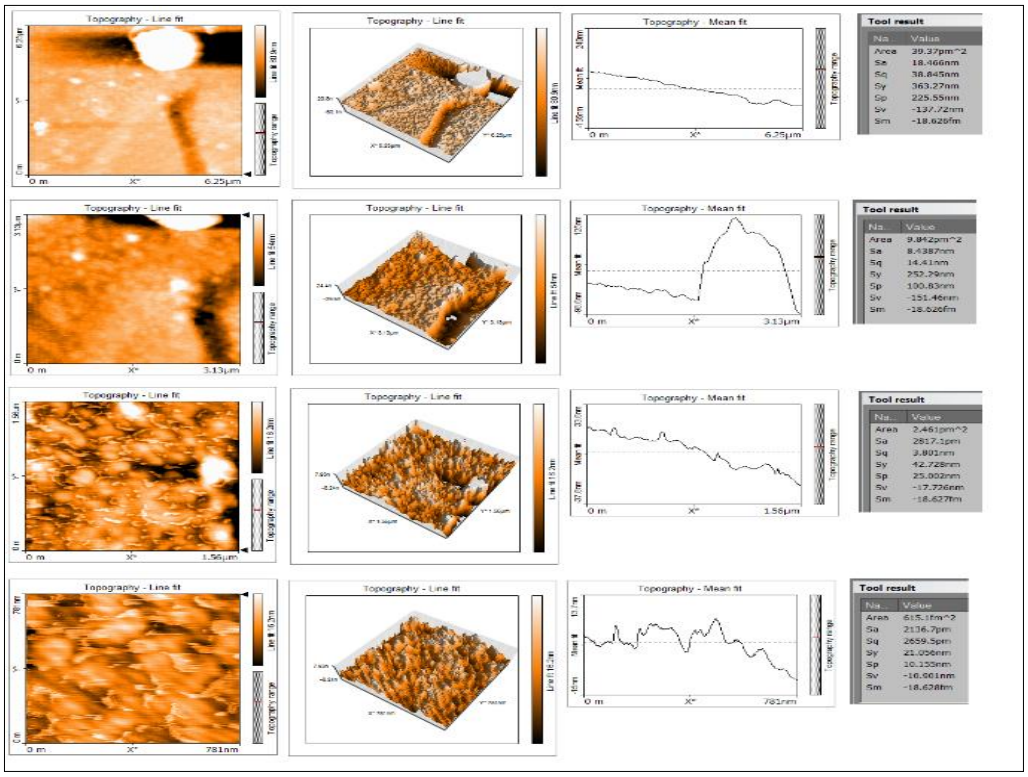

Figure 3 AFM Image of Tellurium Nanoparticles using *Chicoreus virgineus*

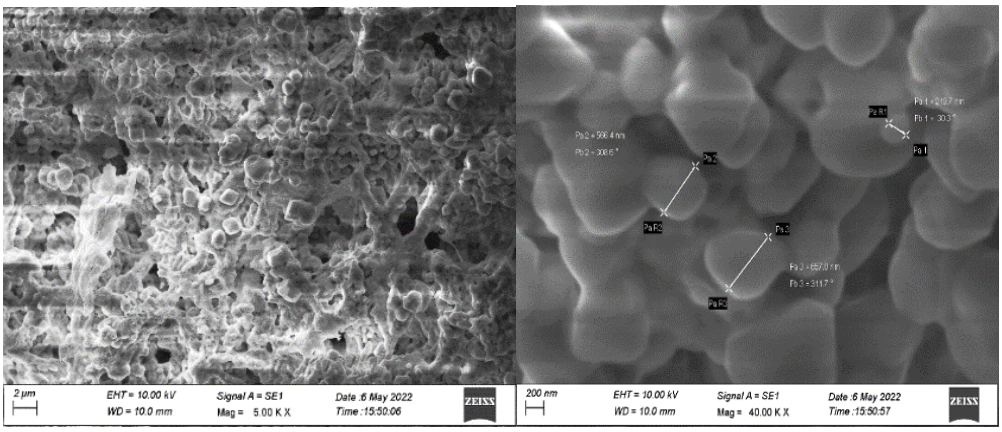

Figure 4 SEM Spectra of Tellurium Nanoparticles using *Chicoreus virgineus*

4.5 X-Ray Diffraction analysis

The quality and particle size of the produced nanoparticles were evaluated using XRD. X-ray diffraction is one of the most popular techniques for characterising NPs (XRD). XRD typically reveals the lattice parameters, phase, crystalline grain size, and crystalline structure. The latter parameter is computed using the Scherrer equation and the broadening of the strongest peak of an XRD measurement for a specific sample. Utilizing XRD methods has the benefit of generating statistically representative, volume-averaged results. These methods are routinely applied to powdered samples, usually following drying of the related colloidal solutions (Mourdikoudis, Pallares, & Thanh, 2018). From Figure 5, the particle was calculated. The crystallite size of the particle was found to be 21.31 nm and it was calculated using the formula $L = 0.89 \lambda / (B \cos \theta)$. Upadhyay, Parekh, & Pandey (2016) reported by utilising X-ray line broadening, the typical crystallite size of magnetite NPs was discovered to be between 9 and 53 nm. Other than experimental broadening, particle/crystallite size and lattice stresses were the main causes of the broadening of XRD peaks. Li et al., (2013) found that the relative intensities between the various XRD peaks changed depending on the shape of the particle after creating copper telluride nanostructures in a variety of shapes (such as cubes, plates, and rods).

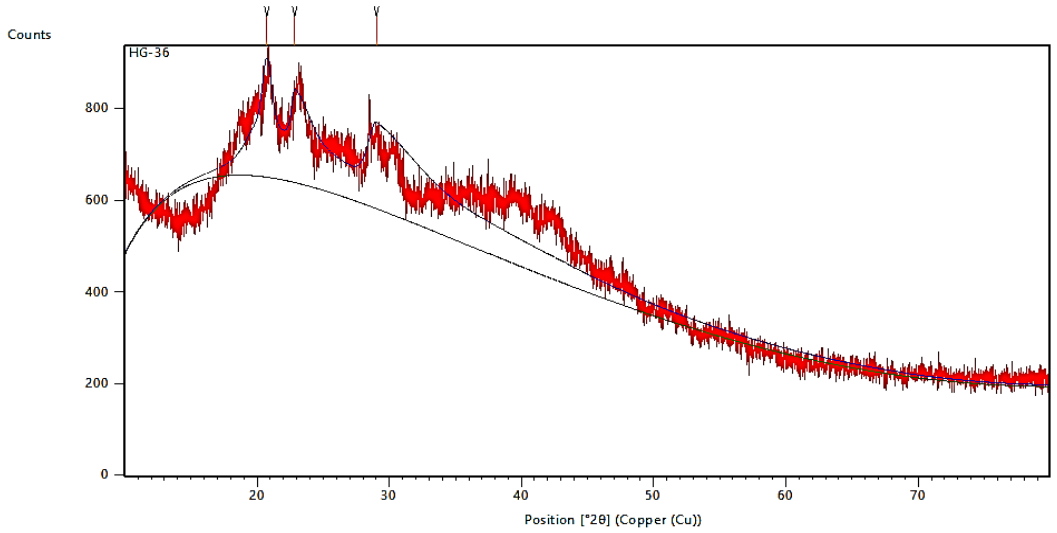

Figure 5 XRD pattern of Tellurium Nanoparticles using *Chicoreus virgineus*

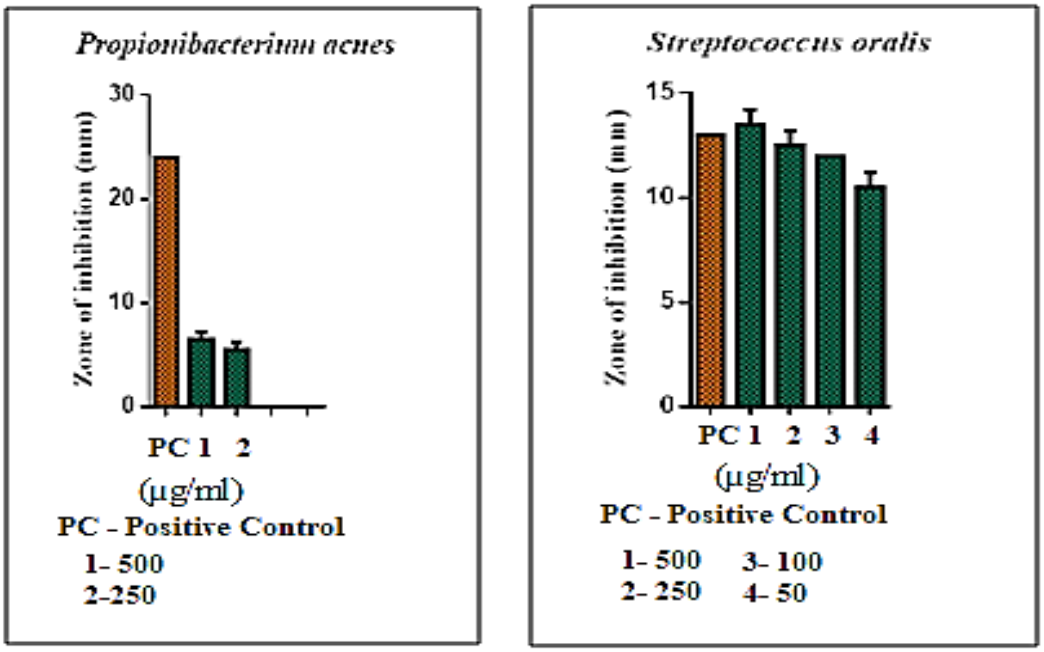

Figure 6 Antibacterial activity of Tellurium Nanoparticles using *C. virgineus* against *Propionibacterium acnes* and *Streptococcus oralis*

4.6 Antibacterial activity of Tellurium nanoparticles

In *C. virgineus* the antibacterial activity of tellurium nanoparticles showed maximum zone of inhibition against *Propionibacterium acnes* at the level of 6.5 mm at 500 µg/mL concentration followed by 5.5 mm at 250 µg/mL concentration. In *Streptococcus oralis* at the level of 13.5 mm at 500 µg/mL concentration followed by 12.5 mm at 250 µg/mL concentration respectively (Figure 6). Similar to the present study Brown, Cruz, Roy and Webster (2018) studied the PVP-coated tellurium nanorods, as well as their antibacterial efficacy against methicillin-resistant Staphylococcus aureus and multidrug-resistant *Escherichia coli*. Vennila, Chitra, Balagurunathan, & Palvannan (2018) analyzed the antibacterial, anticancer and anti-inflammatory activity of SeNPs biofabricated by *Spermacoce hispida* and functionalized with apigenin, quinoline, quinazoline and synaptogenin B. TeNPs have been shown to possess antibacterial, antioxidant, antifungal, and anticancer effects. Khalef, Marzoog, & Faisal (2021) reported tellurium oxide nanoparticles synthesis, characterisation and tested its antibacterial efficacy against strains of *E. coli*, *Proteus vulgaris*, *Pseudomonas*and *Staphylococcus aureus.*

4.7 Antifungal activity of Tellurium nanoparticles

In *C. virgineus* the antifungal activity of tellurium nanoparticles showed maximum zone of inhibition against *Aspergillus fumigatus* at the level of 16.5 mm at 500 µg/mL concentration followed by 12.5 mm at 250 µg/mL concentration. *Cryptococcus neoformans* at the level of 14.5 mm at 500 µg/mL concentration followed by 11.25 mm at 250 µg/mL concentration, respectively (Figure 7). It has been reported that antifungal effect was dose dependent.

Different types of silver nanoparticles, such as those against *Candida* spp. and dermatophytes, are known to show antifungal action against clinical isolates of human infections (Panáček et al., 2009). When tested on the *Candida albicans* BWP17 isolate, a different form of silver nanoparticle produced through biosynthesis and stabilised with starch was found to have strong antifungal action, with a minimum inhibitory concentration (at 80% inhibition, MIC80) of 280 g/mL (Prasher, Singh, & Mudila, 2018). Moreover, another study reveals the antimicrobial and anticancer properties of citrus juice-mediated synthesized TeNPs (Medina Cruz, Mi, & Webster, 2018). To combat potential human infections, the *S. baltica* synthesized TeNRs shows strong

photocatalytic and anti-biofilm action (Vaigankar, Dubey, Mujawar, D'Costa, & Shyama, 2018). Jin et al., (2020) prepared black fungus-extracted BFP nanotubes (triple helix -(1,3)-D-glucan) with hydrophilic hydroxyl groups contain SeNPs embedded and uniformly scattered. Interesting cytotoxic and antitumor characteristics were displayed by these nanocomposites.

4.8 Antioxidant activity

4.8.1 DPPH radical scavenging activity

The DPPH radical scavenging activity of marine molluscan shell extract of *C. virgineus* was observed at various concentrations of 500 µg/mL, 250 µg/mL, 100 µg/mL, 50 µg/mL and 10 µg/mL respectively. The highest percentage inhibition of 71.4% was observed at 500 µg/mL followed by 67.85% at 250 µg/mL, 64.31% at 100 µg/mL, 62.88% at 50 µg/mL and 59.78% at 10 µg/mL respectively. The percentage inhibition of 87.73% was found as the standard ascorbic acid. The IC_{50} value of 121.7 µg/mL was noted which shows the good antioxidant activity. It has been found that antioxidant activity was dose dependent and the percentage inhibition was found to increase with increase in the concentration respectively (Figure 8).

Similar to the present report Kharat, and Mendhulkar (2016) examined the antioxidant potentials of photosynthesized nanoparticles and reported the antioxidant activity of produced nanoparticles using the DPPH assay. Priya, Geetha, & Ramesh (2016) observed the biosynthesized nanoparticles from *P. pinnata* extract and tested for *in vitro* antioxidant activity and shown to have high free radical scavenging capacity. Patra, and Baek (2016) revealed excellent antioxidant activity in terms of scavenging DPPH radicals (IC_{50} 385.87 µg/mL). Shakibaie et al., (2017) described the antibacterial and antioxidant capabilities of tellurium nanorods (TeNRs) produced biologically.

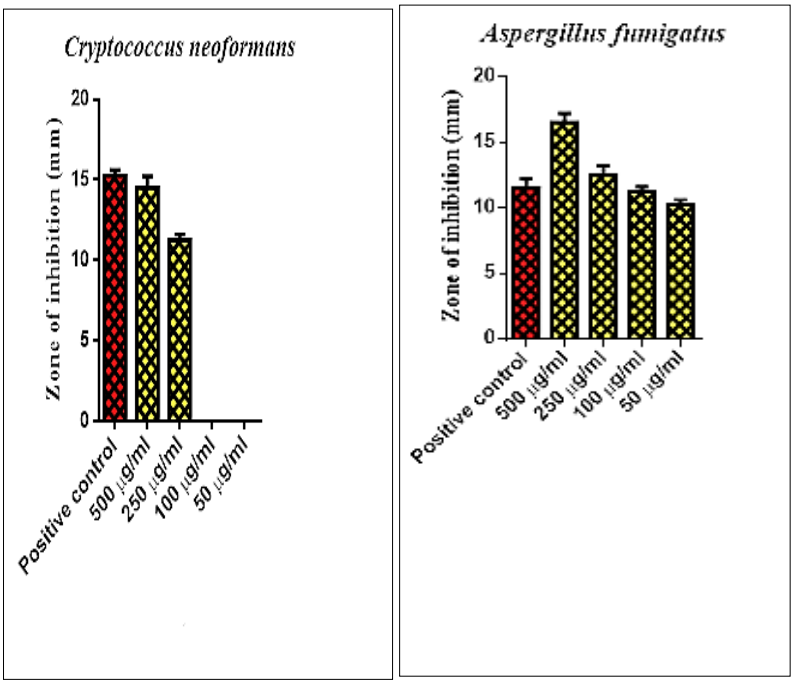

Figure 7 Antifungal activity of Tellurium Nanoparticles using *C. virgineus* against *Cryptococcus neoformans* and *Aspergillus fumigatus*

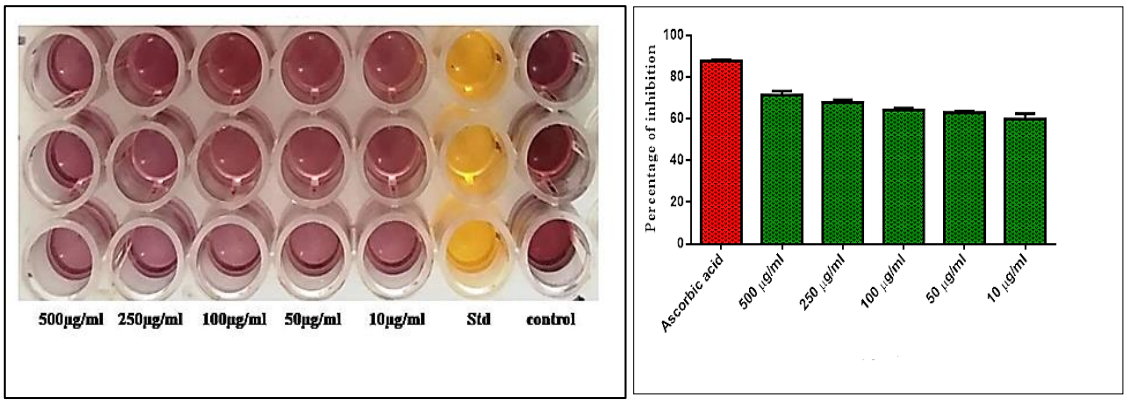

Figure 8 DPPH scavenging assay of Tellurium nanoparticles using *C.virgineus*

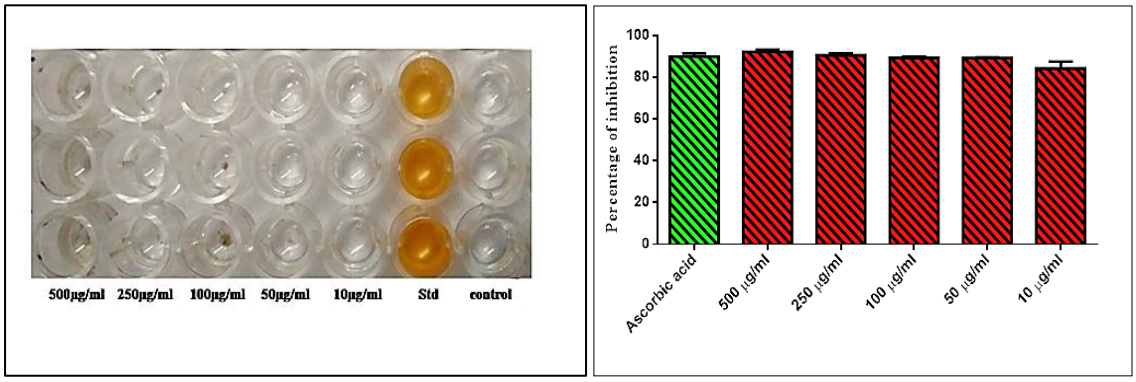

Figure 9 H_2O_2 scavenging activity of Tellurium nanoparticles using *C. virgineus*

4.8.2 Hydrogen Peroxide scavenging assay

The hydrogen peroxide scavenging assay of marine molluscan shell extract of *C. virgineus* was observed at various concentrations of 500 µg/mL, 250 µg/mL, 100 µg/mL, 50 µg/mL and 10 µg/mL respectively. The highest percentage of inhibition of 92.12% was observed at 500 µg/mL followed by 90.55% at 250 µg/mL, 89.23% at 100 µg/mL, 89.09% at 50 µg/mL and 84.23% at 10 µg/mL respectively. The percentage of inhibition of 89.95% was found as the standard ascorbic acid. The IC_{50} value of 51.06 µg/mL was noted which shows the good antioxidant activity. It has been found that antioxidant activity was dose dependent and the percentage inhibition was found to increase with increase in the concentration respectively (Figure 9). Mosallam, El-Sayyad, Fathy, & El-Batal (2018) combined-rays and the *A. oryzae* supernatant to create SeNPs and discovered a substantial association between the antioxidant potential and the phenolic content as well as SeNP production. Gao et al., (2020) revealed the lower risk of selenium toxicity and explored the antioxidant abilities of SeNPs

5. Conclusion

Biosynthetic methods of synthesizing nanoparticles provide a new possibility of conveniently using natural reducing and stabilizing agents. In the present study tellurium nanoparticles were synthesized using the marine gastropod shell *Chicoreus virgineus*. The synthesized tellurium nanoparticles showed good rod shape and surface morphology with crystallite size of 21.31 nm. It was observed that the tellurium nanoparticles showed potent biological properties like antibacterial, antifungal and antioxidant activities. It has been observed that antimicrobial activities were dose dependent and the zone of inhibition found to increase with increase in the concentration. The IC_{50} value of 121.7 µg/mL and 51.06 µg/mL was noted for DPPH scavenging and hydrogen peroxide activity. Tellurium nanoparticles synthesized from these species is a cheaper method. The shell of *C. virgineus* is available in the sea shore and it is affordable. So, producing nanoparticles from these species is a cheaper biogenic approach. In the current scenario developing a good therapeutic applicator is

attractive among the researchers. These highlighted nanoparticles with enriched applications will prove as a good antimicrobial and antioxidant applicators.

6. References

Bartosiak, M., Giersz, J., Jankowski, K. (2019). Analytical monitoring of selenium nanoparticles green synthesis using photochemical vapor generation coupled with MIP-OES and UV–Vis spectrophotometry. *Microchemical Journal*, *145*, 1169-1175. https://doi.org/10.1016/j.microc.2018.12.024

Brown, C. D., Cruz, D. M., Roy, A. K., & Webster, T. J. (2018). Synthesis and characterization of PVP-coated tellurium nanorods and their antibacterial and anticancer properties. *Journal of Nanoparticle Research*, *20*, 1-13. https://doi.org/10.1007/s11051-018-4354-8

Choi, W., Ha, Y., Gu, Y., Lee, C., Park, J., Jang, G., ... & Cho, S. (2019). Microbial tellurite reduction and production of elemental tellurium nanoparticles by novel bacteria isolated from wastewater. *Journal of Industrial and Engineering Chemistry*, *78*, 246-256. https://doi.org/10.1016/j.jiec.2019.06.006

Cui, D., Liang, T., Sun, L., Meng, L., Yang, C., Wang, L., ... & Li, Q. (2018). Green synthesis of selenium nanoparticles with extract of hawthorn fruit induced HepG2 cells apoptosis. *Pharmaceutical biology*, *56*(1), 528-534. https://doi.org/10.1080/13880209.2018.1510974

Diko, C. S., Zhang, H., Lian, S., Fan, S., Li, Z., & Qu, Y. (2020). Optimal synthesis conditions and characterization of selenium nanoparticles in *Trichoderma* sp. WL-Go culture broth. *Materials Chemistry and Physics*, *246*, Article 122583. https://doi.org/10.1016/j.matchemphys.2019.122583

De Magaldi, S. W., & Camero, T. (1997). Suceptibilidad de Candida albicans *In vitro* mediante los posos de difusión. *Bol. venez. infectol*, *7*(1), 5-8. Retrieved from https://pesquisa.bvsalud.org/portal/resource/pt/lil-212701

El-Sayyad, G. S., El-Bastawisy, H. S., Gobara, M., & El-Batal, A. I. (2020). Gentamicin-assisted mycogenic selenium nanoparticles synthesized under gamma irradiation for robust reluctance of resistant urinary tract infection-causing pathogens. *Biological trace element research*, *195*, 323-342. https://doi.org/10.1007/s12011-019-01842-z

Estevam, E. C., Griffin, S., Nasim, M. J., Denezhkin, P., Schneider, R., Lilischkis, R., ... & Jacob, C. (2017). Natural selenium particles from Staphylococcus carnosus: Hazards or particles with particular promise? *Journal of hazardous materials*, *324*, 22-30. https://doi.org/10.1016/j.jhazmat.2016.02.001

Fan, D., Li, L., Li, Z., Zhang, Y., Ma, X., Wu, L., ... & Guo, F. (2020). Biosynthesis of selenium nanoparticles and their protective, antioxidative effects in streptozotocin induced diabetic rats. *Science and technology of advanced materials*, *21*(1), 505-514. https://doi.org/10.1080/14686996.2020.1788907

Fernández-Llamosas, H., Castro, L., Blázquez, M. L., Díaz, E., & Carmona, M. (2016). Biosynthesis of selenium nanoparticles by Azoarcus sp. CIB. *Microbial cell factories*, *15*(1), 1-10. https://doi.org/10.1186/s12934-016-0510-y

Figueroa, M., Fernandez, V., Arenas-Salinas, M., Ahumada, D., Muñoz-Villagrán, C., Cornejo, F., ... & Arenas, F. (2018). Synthesis and antibacterial activity of metal (loid) nanostructures by environmental multi-metal (loid) resistant bacteria and metal (loid)-reducing flavoproteins. *Frontiers in Microbiology*, *9*, Article 959. https://doi.org/10.3389/fmicb.2018.00959

Fissan, H., Ristig, S., Kaminski, H., Asbach, C., & Epple, M. (2014). Comparison of different characterization methods for nanoparticle dispersions before and after aerosolization. *Analytical Methods*, *6*(18), 7324-7334. https://doi.org/10.1039/C4AY01203H

Gao, X., Li, X., Mu, J., Ho, C. T., Su, J., Zhang, Y., & Xie, Y. (2020). Preparation, physicochemical characterization, and anti-proliferation of selenium nanoparticles stabilized by *Polyporusum bellatus* polysaccharide. *International journal of biological macromolecules*, *152*, 605-615. https://doi.org/10.1016/j.ijbiomac.2020.02.199

Gülcin, İ. (2006). Antioxidant and antiradical activities of L-carnitine. *Life sciences*, *78*(8), 803-811. https://doi.org/10.1016/j.lfs.2005.05.103

Hu, T., Li, H., Li, J., Zhao, G., Wu, W., Liu, L., ... & Guo, Y. (2018). Absorption and bio-transformation of selenium nanoparticles by wheat seedlings (*Triticumaestivum* L.). *Frontiers in Plant Science*, *9*, 597. https://doi.org/10.3389/fpls.2018.00597

Jawad, N. A., & Hassan, K. H. (2021). Structural Characterization of NiO NanoparticlesPrepared by Green Chemistry Synthesis using *Arundodonaxi* Leaves Extract. *Journal of Physics: Conference Series*, *1818*(1), 012007, https://doi.org/10.1088/1742-6596/1818/1/012007

Jin, Y., Cai, L., Yang, Q., Luo, Z., Liang, L., Liang, Y., ... & Zhou, F. (2020). Anti-leukemia activities of selenium nanoparticles embedded in nanotube consisted of triple-helix β-D-glucan. *Carbohydrate polymers*, *240*, 116329. https://doi.org/10.1016/j.carbpol.2020.116329

Khalef, W. K., Marzoog, T. R., & Faisal, A. D. (2021). Synthesis and characterization of tellurium oxide nanoparticles using pulse laser ablation and study their antibacterial activity. *Journal of Physics: Conference Series*, *1795*(1), 012049. https://doi.org/10.1088/1742-6596/1795/1/012049

Kharat, S. N., &Mendhulkar, V. D. (2016). Synthesis, characterization and studies on antioxidant activity of silver nanoparticles using Elephantopus scaber leaf extract. *Materials Science and Engineering: C*, *62*, 719-724. https://doi.org/10.1016/j.msec.2016.02.024

Khoei, N. S., Lampis, S., Zonaro, E., Yrjälä, K., Bernardi, P., &Vallini, G. (2017). Insights into selenite reduction and biogenesis of elemental selenium nanoparticles by two environmental isolates of *Burkholderia fungorum*. *New biotechnology*, *34*, 1-11. https://doi.org/10.1016/j.nbt.2016.10.002

Li, W., Zamani, R., Rivera Gil, P., Pelaz, B., Ibáñez, M., Cadavid, D., ... & Cabot, A. (2013). CuTe nanocrystals: shape and size control, plasmonic properties, and use as SERS probes and photothermal agents. *Journal of the American Chemical Society*, *135*(19), 7098-7101. https://doi.org/10.1021/ja401428e

Lian, S., Diko, C. S., Yan, Y., Li, Z., Zhang, H., Ma, Q., & Qu, Y. (2019). Characterization of biogenic selenium nanoparticles derived from cell-free extracts of a novel yeast Magnusiomyces ingens. *3 Biotech*, *9*, 1-8. https://doi.org/10.1007/s13205-019-1748-y

Liang, T., Qiu, X., Ye, X., Liu, Y., Li, Z., Tian, B., & Yan, D. (2020). Biosynthesis of selenium nanoparticles and their effect on changes in urinary nanocrystallites in calcium oxalate stone formation. *3 Biotech*, *10*, 1-6. https://doi.org/10.1007/s13205-019-1999-7

Medina Cruz, D., Mi, G., & Webster, T. J. (2018). Synthesis and characterization of biogenic selenium nanoparticles with antimicrobial properties made by Staphylococcus aureus, methicillin-resistant Staphylococcus aureus (MRSA), Escherichia coli, and Pseudomonas aeruginosa. *Journal of Biomedical Materials Research Part A*, *106*(5), 1400-1412. https://doi.org/10.1002/jbm.a.36347

Mosallam, F. M., El-Sayyad, G. S., Fathy, R. M., & El-Batal, A. I. (2018). Biomolecules-mediated synthesis of selenium nanoparticles using Aspergillus oryzae fermented Lupin extract and gamma radiation for hindering the growth of some multidrug-resistant bacteria and pathogenic fungi. *Microbial pathogenesis*, *122*, 108-116. https://doi.org/10.1016/j.micpath.2018.06.013

Mourdikoudis, S., Pallares, R. M., & Thanh, N. T. (2018). Characterization techniques for nanoparticles: comparison and complementarity upon studying nanoparticle properties. *Nanoscale*, *10*(27), 12871-12934. https://doi.org/10.1039/C8NR02278J

Mulla, N. A., Otari, S. V., Bohara, R. A., Yadav, H. M., & Pawar, S. H. (2020). Rapid and size-controlled biosynthesis of cytocompatible selenium nanoparticles by Azadirachta indica leaves extract for antibacterial activity. *Materials Letters*, *264*, 127353. https://doi.org/10.1016/j.matlet.2020.127353

Panáček, A., Kolář, M., Večeřová, R., Prucek, R., Soukupová, J., Kryštof, V., ... & Kvítek, L. (2009). Antifungal activity of silver nanoparticles against Candida spp. *Biomaterials*, *30*(31), 6333-6340. https://doi.org/10.1016/j.biomaterials.2009.07.065

Patra, J. K., & Baek, K. H. (2016). Biosynthesis of silver nanoparticles using aqueous extract of silky hairs of corn and investigation of its antibacterial and anticandidal synergistic activity and antioxidant potential. *IET nanobiotechnology*, *10*(5), 326-333. https://doi.org/10.1049/iet-nbt.2015.0102

Prasher, P., Singh, M., &Mudila, H. (2018). Green synthesis of silver nanoparticles and their antifungal properties. *BioNanoScience*, *8*, 254-263. https://doi.org/10.1007/s12668-017-0481-4

Priya, R. S., Geetha, D., & Ramesh, P. S. (2016). Antioxidant activity of chemically synthesized AgNPs and biosynthesized Pongamia pinnata leaf extract mediated AgNPs–A comparative study. *Ecotoxicology and environmental safety*, *134*, 308-318. https://doi.org/10.1016/j.ecoenv.2015.07.037

Ruch, R. J., Cheng, S. J., &Klaunig, J. E. (1989). Prevention of cytotoxicity and inhibition of intercellular communication by antioxidant catechins isolated from Chinese green tea. *Carcinogenesis*, *10*(6), 1003-1008. https://doi.org/10.1093/carcin/10.6.1003

Shakibaie, M., Adeli-Sardou, M., Mohammadi-Khorsand, T., ZeydabadiNejad, M., Amirafzali, E., Amirpour-Rostami, S., ... & Forootanfar, H. (2017). Antimicrobial and antioxidant activity of the biologically synthesized tellurium nanorods; a preliminary in vitro study. *Iranian journal of biotechnology*, *15*(4), 268. https://doi.org/10.15171/ijb.1580

Tanaka, Y. K., Takada, S., Kumagai, K., Kobayashi, K., Hokura, A., & Ogra, Y. (2020). Elucidation of tellurium biogenic nanoparticles in garlic, Allium sativum, by inductively coupled plasma-mass spectrometry. *Journal of Trace Elements in Medicine and Biology*, *62*, 126628. https://doi.org/10.1016/j.jtemb.2020.126628

Tugarova, A. V., Mamchenkova, P. V., Khanadeev, V. A., & Kamnev, A. A. (2020). Selenite reduction by the rhizobacterium Azospirillum brasilense, synthesis of extracellular selenium nanoparticles and their characterisation. *New biotechnology*, *58*, 17-24. https://doi.org/10.1016/j.nbt.2020.02.003

Upadhyay, S., Parekh, K., & Pandey, B. (2016). Influence of crystallite size on the magnetic properties of Fe3O4 nanoparticles. *Journal of Alloys and Compounds*, *678*, 478-485. https://doi.org/10.1016/j.jallcom.2016.03.279

Vaigankar, D. C., Dubey, S. K., Mujawar, S. Y., D'Costa, A., & Shyama, S. K. (2018). Tellurite biotransformation and detoxification by Shewanellabaltica with simultaneous synthesis of tellurium nanorods exhibiting photo-catalytic and anti-biofilm activity. *Ecotoxicology and environmental safety*, *165*, 516-526. https://doi.org/10.1016/j.ecoenv.2018.08.111

Vennila, K., Chitra, L., Balagurunathan, R., & Palvannan, T. (2018). Comparison of biological activities of selenium and silver nanoparticles attached with bioactive phytoconstituents: green synthesized using Spermacocehispida extract. *Advances in Natural Sciences: Nanoscience and Nanotechnology*, *9*(1), 015005. https://doi.org/10.1088/2043-6254/aa9f4d

Wang, K., Zhang, X., Kislyakov, I. M., Dong, N., Zhang, S., Wang, G., ... & Wang, J. (2019). Bacterially synthesized tellurium nanostructures for broadband ultrafast nonlinear optical applications. *Nature Communications*, *10*(1), 3985. https://doi.org/10.1038/s41467-019-11898-z

Zhang, D., Ma, X. L., Gu, Y., Huang, H., & Zhang, G. W. (2020). Green synthesis of metallic nanoparticles and their potential applications to treat cancer. *Frontiers in Chemistry*, *8*, 799. https://doi.org/10.3389/fchem.2020.00799